

**Structural Characterization by Scattering and Spectroscopic Methods and
Biological Evaluation of Polymeric Micelles of Poloxamines and TPGS as
Nanocarriers for Miltefosine Delivery**

Joan Puig-Rigall^a, Celia Fernandez-Rubio^b, Javier González-Benito^c, Judith E.
Houston^d, Aurel Radulescu^d, Paul Nguewa^{b,*}, Gustavo González-Gaitano^{a,*}

^a Departamento de Química, Facultad de Ciencias, Universidad de Navarra, 31080
Pamplona, SPAIN

^b University of Navarra, ISTUN Instituto de Salud Tropical, Department of
Microbiology and Parasitology. Irunlarrea 1, 31008 Pamplona, SPAIN

^c Department of Materials Science and Engineering, IQMAAB, Universidad Carlos III
de Madrid, Av. Universidad 30, 28911 Leganés, SPAIN

^d Jülich Centre for Neutron Science (JCNS) at Heinz Maier-Leibnitz Zentrum (MLZ),
Forschungszentrum Jülich GmbH, Lichtenbergstraße 1, 85747 Garching, Germany

*Corresponding authors: gaitano@unav.es, panguewa@unav.es

Abstract

Miltefosine (MF), an alkylphospholipid originally developed for breast cancer treatment, is a highly active drug for the treatment against leishmaniasis, a neglected tropical disease considered the world's second leading cause of death by a parasitic agent after malaria. MF exhibits dose-limiting gastrointestinal side effects in patients and its penetration through lipophilic barriers is reduced. In this work we propose a reformulation of MF by incorporating the drug to poly(ethylene)oxide (PEO)-based polymeric micelles, specifically, D- α -tocopheryl polyethylene glycol succinate (TPGS) and Tetronic block copolymers (T904 and T1107). A full structural characterization of the aggregates has been carried out by SANS (small-angle neutron scattering) and dynamic light scattering (DLS), in combination with proton 1D and 2D NMR spectroscopy, to determine the precise location of the drug. The structure of MF micelles has been characterized as a function of the temperature and concentration. In the presence of the polymers, MF forms mixed micelles in a wide range of temperatures, TPGS being the co-surfactant that incorporates more MF unimers. The hydrophobic parts of MF and the block copolymers are in close contact within the micelles, which present a core-shell structure with a hydrophilic corona formed by the PEG blocks of the TPGS and the zwitterion head of the MF. With the aim of exploring gel-based formulations of the drug, the combination of MF and T1107 under gelation conditions has also been investigated. In order to identify the best carrier, the antileishmanicidal activity of MF in the different formulations has been tested on macrophages, promastigotes and intracellular amastigotes. The combination of the three vehicles with MF makes the formulated drug more active than MF alone against *L. major* promastigotes, however, only the combination with T904 increases the MF activity against intracellular amastigotes.

Keywords: miltefosine, Tetronic, poloxamine, TPGS, micelles, gels, cytotoxicity, SANS

1. INTRODUCTION

Leishmaniasis is a group of diseases caused by parasites of the *Leishmania* genus transmitted by female sand flies. Different clinical forms of the leishmaniasis are known, being the cutaneous leishmaniasis (CL) the most common form of the disease.^{1,2} A large number of antitumoral compounds have demonstrated activity to treat the disease,^{3,4} although the only oral drug reported to have an effect against *Leishmania* parasite is miltefosine (MF), an alkylphospholipid originally developed for breast cancer treatment.^{5,6} When compared to the current first-line therapies, MF is more cost-effective,⁷ and several studies have suggested its application against leishmaniasis using different formulations.^{8–15} However, it exhibits dose-limiting gastrointestinal side effects in patients¹⁶ and MF penetration through lipophilic barriers is reduced,¹⁷ drawbacks that can be overcome by using nanocarriers, like liposomes¹⁸.

Polymeric micelles based on poly(ethylene)oxide (PEO) are promising drug carrier candidates, as they meet a number of key requirements, in terms of structure (distinct core-shell architecture providing physical entrapment of hydrophobic drugs; hydrophilic PEO corona reducing recognition by macrophages) and size (just a few nanometers). Recent studies have described MF-loaded polymeric micelles of Pluronic® surfactants,^{19,20} linear triblock copolymers of poly(ethylene oxide)-poly(propylene oxide)-poly(ethylene oxide) (PEO-PPO-PEO) that differ in the relative length of PEO and PPO blocks, giving different micellization and gel-transition behaviour depending on the temperature.^{21–23}

In this work we have considered two types of block copolymers based on PEO as potential carriers of MF. The first one is D- α -tocopheryl polyethylene glycol succinate, TPGS, a water-soluble derivative of the natural form of vitamin E, where the D- α -tocopheryl succinate is esterified with a short polyethylene glycol (PEG) chain.²⁴ It has been approved by the Food and Drug Administration (FDA) and investigated for its capacity to solubilize hydrophobic substances for drug delivery.^{25,26} TPGS forms core-shell micelles with a *cmc* of 0.02% and $N_{agg} \approx 100$, and a highly hydrated PEO corona, very stable with the temperature and concentration.²⁷ The other type of block copolymers studied are poloxamines, also known by their commercial name of Tetronic® (BASF). These polymeric surfactants are octablock copolymers of PEO and PPO, distributed into four arms connected by a central ethylene diamine spacer. They share the amphiphilic character and self-assembly behaviour with the well-known and broadly utilised Pluronic® family, forming micelles and gels as a function of temperature and concentration. However, in contrast, they are pH-responsive, which dramatically affects the micellization and gelation of the block copolymer and, thus, can be used to release a cargo upon a pH-trigger.^{28–31} Specifically, we have investigated the structures formed when TPGS and Tetronic 904 (T904) and 1107 (T1107) are combined with MF. These poloxamines were chosen considering their molar mass and HLB, as T904 is relatively small and lipophilic, while the larger T1107 can form gels under certain conditions.

The polymeric mixed micelles formed between MF and the different carriers have been characterized by scattering methods, such as small-angle neutron scattering (SANS) and dynamic light scattering (DLS), to determine the structure of the aggregates and their composition, while proton 1D and 2D NMR spectroscopy has been used to determine the precise location of the drug in the aggregates. To the best of our knowledge, this is the first time micelles of MF at different temperature and concentrations have been fully

characterized using these methods. The combination of MF and T1107 under gelation conditions has also been investigated, with the aim of exploring gel-based formulations of MF for potential applications for the treatment of CL. Finally, biological studies in promastigotes and amastigotes were performed, testing the activity of MF in the different formulations to identify the most promising carrier.

2. MATERIALS AND METHODS

2.1 Materials. Tetronic 904 (T904) and 1107 (T1107) were a gift from BASF. The composition per arm of T904 is 15 EO and 17 PO, with average molecular weight of 6700 g mol⁻¹. The composition per arm of T1107 is 60 EO and 20 PO (average molecular weight of 15000 g mol⁻¹). D- α -tocopheryl polyethylene glycol succinate (TPGS) was a gift from Antares Health Products Inc, with a reported PEG molecular weight of 1000 (23 EO units). All the solutions were prepared by weight, and the concentrations are expressed in wt%, unless stated otherwise. Our reference drug miltefosine (MF) was purchased from Sigma-Aldrich.

2.2 Small-angle neutron scattering (SANS). SANS experiments were carried out on the KWS-2 diffractometer at the Jülich Centre for Neutron Science (JCNS), Munich, Germany.³² An incidental wavelength of 5 Å was used with detector distances of 1.7 and 7.6 m, with a collimation length of 8 m, to cover the q range from 0.008 to 0.5 Å⁻¹. In the diluted regime a wavelength spread $\Delta\lambda/\lambda = 20\%$ was used, while in the concentrated regime, a high-resolution mode was achieved by using a collimation length of 20 m in combination with the double-disc chopper and time-of-flight data acquisition for an improved wavelength spread of $\Delta\lambda/\lambda = 5\%$. All samples were measured in rectangular quartz cells (Hellma) with a path length of 2 mm using D₂O as the solvent (Aldrich, 99.9% in D). The samples were placed in an aluminium rack where water was recirculated from

an external Julabo circulator, ranging temperatures from 20 °C to 50 °C. This set-up enables a thermal control with up to 0.1 °C precision. Scattered intensities were corrected for detector pixel efficiency, empty cell scattering and background due to electronic noise. The data were set to absolute scale using Plexiglas as a secondary standard. The obtained macroscopic differential cross-section $d\Sigma/d\Omega$ was further corrected for the contribution from the solvent. The complete data reduction process was performed with the QtiKWS software provided by JCNS in Garching. Data analysis was carried out with Sasview 4.2.0 software (<http://www.sasview.org/>) considering the instrumental smearing. Levenberg-Marquardt algorithm was chosen in each case prior to an in-depth study using the implemented optimizer DREAM, in order to better estimate the uncertainties of the fitted parameters. The scattering curves from the micelles were fitted to a core-shell sphere (CSS) model combined with a hard-sphere (HS) structure factor, while the analysis of the gels scattering was carried out using a body-centred cubic paracrystalline model (BCC).

2.3 Dynamic light scattering (DLS). DLS measurements were carried out using a DynaPro-MS/X photon correlation spectrometer with a laser wavelength of 822 nm at a fixed scattering angle of 90°. The temperature was controlled with the built-in Peltier unit, with 0.1 °C accuracy. The intensity size distributions were obtained from the autocorrelation function, considering the viscosities and refractive indexes of the solvent at each temperature (D₂O, to reproduce SANS conditions) with the implemented software Dynamics V6. Samples were filtered through 0.22 µm PVDF syringe filters prior to the measurements. The samples for the experiments with MF alone were filtered through 0.02 µm filters.

2.4 Nuclear Magnetic Resonance Spectroscopy (NMR). Both 1D and 2D-NOESY proton spectra were recorded on a Bruker Avance Neo 400 spectrometer, using the default pulse sequences for each type of experiment. The temperature in the probe was controlled

according to the sample type. The samples were prepared in D₂O (Aldrich>99.9% in deuterium).

2.5 Biological evaluation

2.5.1 Cells and culture conditions

Leishmania major promastigotes (Lv39c5) were grown at 26 °C in M199 medium supplemented with 25 mM HEPES (pH 7.2), 0.1 mM adenine, 0.0005% (wt/vol) hemin, 2 mg/ml biopterin, 0.0001% (wt/vol) biotin, 10% (vol/vol) heat-inactivated fetal bovine serum (FBS), and an antibiotic cocktail (50 U/ml penicillin, 50 mg/ml streptomycin). To maintain their infectivity, *Leishmania* cells isolated from infected BALB/c mouse spleen and parasites were maintained in culture for no more than five passages. Murine peritoneal macrophages from 4- to 6-week-old BALB/c mice were used for the study. Animals were inoculated with 2 ml sterile thioglycolate (3%) broth (BD Difco) prior to peritoneal cavity lavage with 5 ml of cold RPMI medium, and macrophages were removed by a syringe. All the procedures involving animals were approved by the Animal Care Ethics Commission of the University of Navarra (approval number: E5-16(068-15E1).

2.5.2 Leishmanicidal activity

2.5.2.1 Activity against promastigotes

To determine the antileishmanial activities of the compounds analyzed in this study, exponentially growing cells (2×10^6 *L. major* promastigotes/ml) were seeded in 96-well plates (100 µl per well) with increasing concentrations of the compounds. Stock aqueous solutions of 0.2% (5mM) MF, 1% Polymer and 1% Polymer + 0.2% MF were diluted in 100 µl of M199 medium (obtaining the corresponding concentrations) and maintained at 26°C. After 72 h of incubation, the half-maximal effective concentration (EC₅₀) was

calculated by the MTT test (Sigma, St. Louis, MO, USA), which was also performed to determine the cytotoxicity of selected compounds in bone-marrow-derived macrophage (BMDM). MTT solutions were prepared at 5 mg/ml in phosphate-buffered saline (PBS), filtered and maintained at -20°C until use. After 72 h of incubation, 100 µg/well of MTT were added and the plates were incubated 4 h under the same conditions. Then, 80 µl of a dimethyl sulfoxide were added to each well to dissolve formazan crystals. The optical density (OD) was measured in a Multiskan EX microplate photometer plate reader at 540 nm and EC₅₀ was calculated. The EC₅₀ represents the concentration that gives half-maximal viability of treated cells with respect to untreated cells (controls). This parameter was obtained by fitting a sigmoidal Emax model to dose-response curves.

2.5.2.2 Activity against intracellular amastigotes

Murine peritoneal macrophages were seeded in 8-well culture chamber slides (Lab-Tek™; BD Biosciences) at a density of 5x10⁴ cells per well in Roswell Park Memorial Institute (RPMI) medium and allowed to adhere overnight at 37 °C in a 5% CO₂ incubator. In order to perform the infection assay, metacyclic *L. major* promastigotes isolated by the peanut agglutinin (PNA) method were used to infect macrophages at a macrophage/parasite ratio of 1/20. The plates were incubated for 24 h under the same conditions until promastigotes were phagocytized by macrophages. The wells were then washed with medium to remove the extracellular promastigotes, and plates were incubated with fresh medium supplemented with increasing concentrations of drug. Dilutions of stock aqueous solutions of 0.2% (5mM) MF, 1% Polymer and 1% Polymer + 0.2% MF were done. Forty-eight hours later, cells were washed with PBS, fixed with ice-cold methanol for 5 min, and stained with Giemsa stain. To determine parasite burden, the number of infected macrophages per at least 200 macrophages was counted under a light microscope. The percentage of infected macrophage was determined by dividing the

total number of infected macrophages counted by the corresponding number of macrophages. Three independent experiments were performed with duplicates.

2.5.3 Statistical analysis

Statistical analyses were performed using PRISM version 5.0 (GraphPad). Data are presented as mean \pm SD. Comparisons between two groups were made using Mann Whitney or two-tailed unpaired t-test. Statistical significance was assigned to $p < 0.001$ (***), $p < 0.01$ (**) or $p < 0.05$ (*).

3. RESULTS AND DISCUSSION

3.1 Characterization of miltefosine micelles

Zwitterionic MF self-aggregates in water forming micelles, whose values of critical micellar concentration (*cmc*) in aqueous solutions vary depending of the technique employed,^{33,34} with reported values between 2 and 15 μM .^{35,36} By using DLS (SI, Figure 1), at 0.2% (5mM) MF, considerably above the reported *cmc*, the presence of micelles of $R_h = 3.5$ nm can be observed at 20 and 37 °C, in accordance with literature values,¹⁹ while slightly smaller sizes are obtained at 50 °C ($R_h = 3.0$ nm). At higher concentration of the surfactant (1%), no temperature effect was observed for the MF micelles, with a hydrodynamic radius of 3.0 nm. Detailed information about the micelle structures can be determined by SANS. The scattering patterns as a function of temperature are plotted in Figure 1, in which the fitted curves to a CSS-HS model are included. The scattering length density (*sld*) values of the core, assumed to consist of the aliphatic chains, has been fixed at $-3.73 \cdot 10^{-7} \text{ \AA}^{-2}$. The aggregation number of the micelles and fraction of water in the shell were obtained following a procedure described elsewhere,²⁷ considering a value of *sld* = $1.30 \cdot 10^{-6} \text{ \AA}^{-2}$ for the hydrophilic head of a MF molecule, in accordance with literature.³⁷

The polydispersity was fixed to 0.15 after examining the size distributions from DLS. All the relevant structural data obtained is gathered in Table 1.

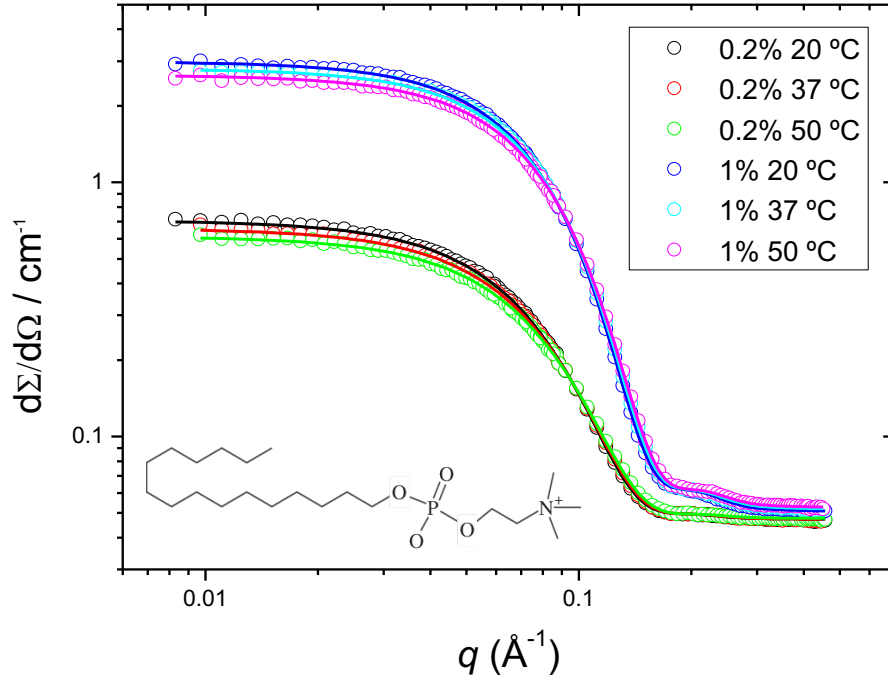


Figure 1. SANS curves of 0.2% and 1% MF in D₂O at 20, 37 and 50 °C. Solid lines correspond to the fits to a CSS-HS model.

Table 1. Structural parameters of MF micelles in D₂O as a function of the temperature, deduced from SANS data analysis. R_c (core radius, Å), t (shell thickness, Å), ϕ (volume fraction), ρ_s (shell scattering length density, $\times 10^6$ Å⁻²), $X_{D_2Oshell}$ (fraction of water in the shell), N_{agg} (aggregation number)

% MF	$T / ^\circ\text{C}$	R_c	t	ϕ	ρ_s	$X_{D_2Oshell}$	N_{agg}
0.2	20	24	7	0.003	5.24	0.779	106
	37	24	6	0.003	5.10	0.751	99
	50	23	7	0.003	5.02	0.735	93
1.0	20	24	8	0.015	5.39	0.808	105
	37	24	8	0.016	5.48	0.826	98
	50	23	7	0.014	5.16	0.763	92

The fitted data reveal a total micelle size, $R_c + t$, of 3 – 3.5 nm, as observed in DLS (SI, Figure 1) for the MF micelles. The micelles are stable with temperature, only but for a slight reduction in their hydration of the shell and aggregation number, N_{agg} , as the temperature increases. No remarkable effects are detected in either the size and or in the N_{agg} with the concentration, but a slightly higher hydration of the shell is observed when increasing from 0.2% to 1%.

3.2 Structure of miltefosine-loaded polymeric micelles

3.2.1 TPGS-MF micelles

The first polymeric surfactant considered as a micellar vehicle for MF is TPGS, which has a *cmc* value of 0.02% and forms stable core-shell micelles in a wide range of temperatures and concentrations.²⁷ The size of 0.2% MF loaded 1% TPGS micelles in D₂O is 5-5.5 nm in radius, as determined by DLS, in agreement with the 5 nm reported for TPGS in water,²⁷ and showing a slight decrease with the temperature (Figure 2). SANS patterns of the mixed system are compared to unloaded 1% TPGS in SI, Figure S2. The resulting curves are quite similar and only differ in a slight reduction in the scattered intensity in the presence of MF and a shift of the curves towards higher q , for all the temperatures investigated, pointing to a reduction in size of the aggregates. The curves have also been fit to a CSS-HS model, but in this case the polydispersity has been left free, obtaining values close to 0.15. Table 2 shows all the relevant structural data obtained.

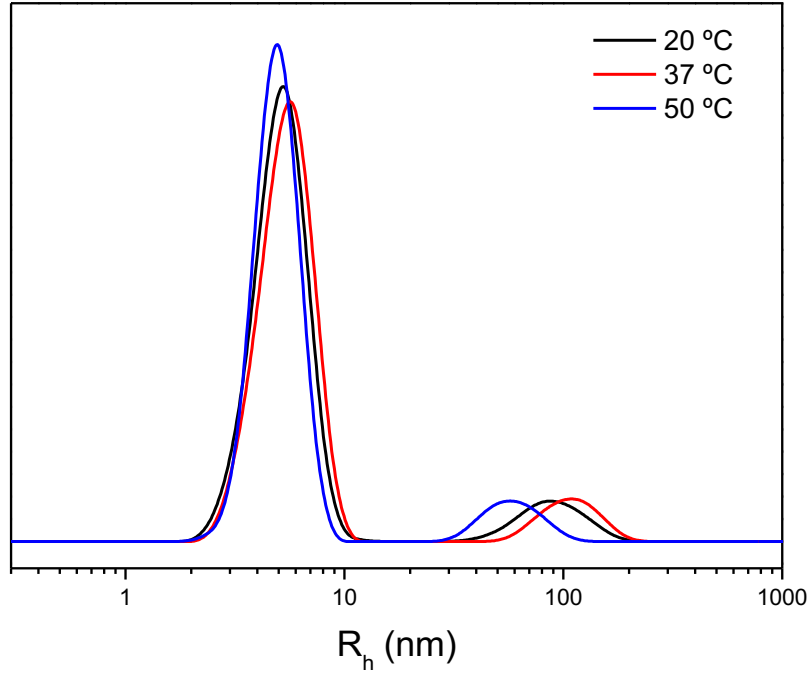


Figure 2. Size distributions obtained by DLS of 1% TPGS + 0.2% MF in D₂O.

Table 2. Structural parameters of TPGS and TPGS-MF mixed micelles in D₂O as a function of the temperature deduced from SANS data analysis. R_c (core radius, Å), t (shell thickness, Å), ϕ (volume fraction), ρ_s (shell scattering length density, $\times 10^6$ Å⁻²), ρ_c (core scattering length density, $\times 10^6$ Å⁻²)

	$T / ^\circ\text{C}$	R_c	t	ϕ	ρ_s	ρ_c
1% TPGS	20	32	30	0.028	5.55	0.28
	37	34	29	0.027	5.65	0.28
	50	35	28	0.026	5.70	0.28
1% TPGS + MF 0.2%	20	31	26	0.035	5.79	0.16
	37	31	24	0.031	5.80	0.03
	50	31	23	0.028	5.80	-0.07

The fits for the TPGS alone were accomplished considering a “dry” core ($sld = 2.8 \times 10^{-7}$ Å⁻², assuming it is formed by tocopherol moieties). The fits reveal highly hydrated shells

and very stable micelles with temperature, in accordance with previous studies.²⁷ The presence of the MF causes the mixed micelle to shrink in size (reduction of *ca.* 11% in total size), and similar sld_s values. However, somewhat lower sld_c are obtained as the temperature increases, which can be attributed to the solubilisation of the hydrophobic part of the MF in the micellar core (for MF $sld_{core} = -3.73 \times 10^{-7} \text{ \AA}^{-2}$).

NMR spectroscopy has proven useful in determining the precise location of drugs dissolved in polymeric micelles.³⁸ Figure 3 shows the aliphatic region of the 1D proton spectrum obtained from a 1% TPGS + 0.2% MF mixture at 25°C, compared with TPGS and MF alone. In the particular case of combined TPGS and MF, both surfactants share similar aliphatic moieties in terms of the NMR signals they produce. Yet, changes on representative protons of both surfactants are observed, which clearly indicate a change in the magnetic environment of the protons upon mixing.

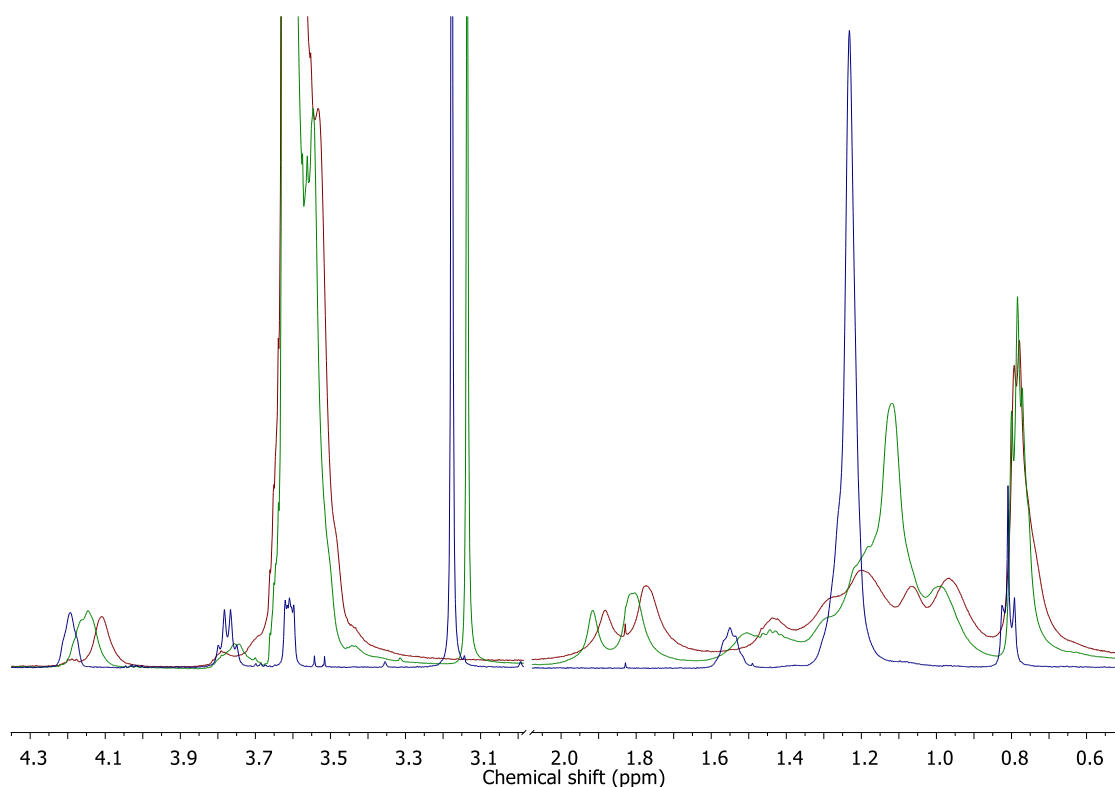


Figure 3. ^1H -NMR spectra in D_2O of 0.2% MF (blue), 1% TPGS (red) and 1% TPGS + 0.2% MF (green) at 25 $^\circ\text{C}$.

The most important changes occur in the methylene protons of the hydrophobic tail of MF (1.23 ppm, see SI, Figure S3 for signal assignment), which shift upfield (1.12 ppm), as well as, to a lesser extent, the CH_3 of the surfactant head (from 3.18 to 3.14 ppm). Changes are also detected in the TPGS protons of the hydrophobic part. Thus, in the aliphatic zone between 1.0 and 1.5 ppm, which corresponds to the resonances of $\text{CH}_3(\text{a})$ and $\text{CH}_2(\text{b})$ of the tocopherol moiety of TPGS,²⁷ protons d and e (directly bonded to the aromatic ring, 1.92 and 1.81 ppm) shift upfield in 0.03 ppm with MF addition. In contrast, the PEG tail of TPGS (intense resonances of the EO residues at 3.64 ppm) remains unaltered. The 2D-NOESY spectrum, shown in Figure 4, helps to define the precise location of both surfactants in the micelles. The lack of any cross-peak between the characteristic CH_3 protons of the zwitterion (3.2 ppm) and any of the tocopherol moiety of TPGS (0.8 – 2.5 ppm) indicates that the MF polar head must be located far from the core. In addition, there is a neat cross-peak between the methyl group of MF with the

aromatic methylene groups, d and e of TPGS. The interactions between these protons and the hydrophobic chain of TPGS are also less intense than those observed in TPGS micelles (SI, Figure 4), which confirms the close proximity of the hydrophobic parts of both surfactants. Overall, the NMR evidence indicates that MF and TPGS are forming a mixed micelle, in which the hydrophobic parts of both surfactants are in close contact, with a hydrophilic shell mainly formed by the PEG blocks of the TPGS and the zwitterion head of the MF.

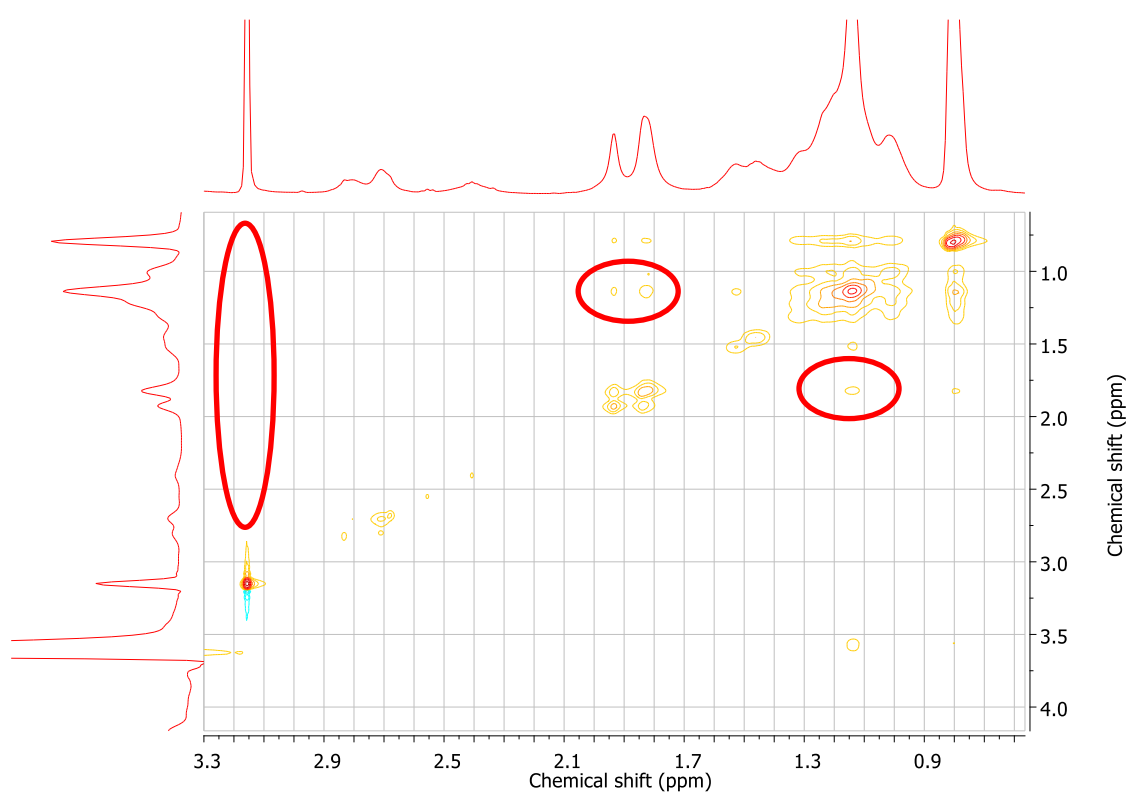


Figure 4. 2D-NOESY spectrum of 1% TPGS + 0.2% MF at 25 °C in D₂O.

By making some reasonable assumptions, it is possible to estimate the content of MF and TPGS in the mixed micelle from the SANS data. Following NMR evidence, the MF tails must be located preferentially in the core, while the shell is formed mostly by the PEG chain. Assuming that the presence of water in the core is negligible, the solvent content

of the micelle comes mainly from the hydration of the EO. The volume of the core (V_c) can be expressed as

$$V_c = v_{TPGS,c} N_{TPGS} + v_{MF,c} N_{MF} \quad (1)$$

where $v_{TPGS,c}$ is the volume of the hydrophobic part of a TPGS molecule, $v_{MF,c}$ that of MF, and N_{TPGS} and N_{MF} the number of molecules of both surfactants per micelle. Likewise, the total volume of the micelle (V_m) is defined as

$$V_m = (v_{TPGS} + n_{EO} n_{solv/EO} v_{D_2O}) N_{TPGS} + v_{MF} N_{MF} \quad (2)$$

where v_{TPGS} and v_{MF} stand for the volume of TPGS and MF molecules, respectively, v_{D_2O} is the volume of a solvent molecule, n_{EO} the number of EO monomers that form the hydrophilic block (23 per TPGS molecule) and $n_{solv/EO}$ the number of solvent molecules per EO monomer. These numbers can be calculated at each temperature if we consider a “pure” TPGS micelle, in which

$$n_{solv} = \frac{\rho_{shell} - \rho_{EO}}{\rho_{D_2O} - \rho_{EO}} \frac{v_{shell}}{v_{D_2O}} \quad (3)$$

where n_{solv} and v_{shell} refer to the number of D₂O molecules in the shell and the volume of the corona of the TPGS micelles, and ρ_{shell} , ρ_{EO} , ρ_{D_2O} correspond to the sld values deduced by SANS (Table 2), the EO ($6.38 \times 10^{-6} \text{ \AA}^{-2}$) and solvent ($6.36 \times 10^{-6} \text{ \AA}^{-2}$). The calculation for this surfactant yields values of $n_{EO} = 10, 9.8$ and 8.8 at $20, 37$ and $50 \text{ }^\circ\text{C}$, respectively, in agreement with our previous studies.²⁷

The number of monomers of TPGS and MF in the micelles can be deduced by solving the simultaneous equations (1) and (2), as well as their volume fractions in the mixed micelles. The results of these calculations are shown in Table 3, where it can be seen how the volume fraction of TPGS in the mixed micelles is always lower than half of the total volume. Interestingly, the combination with TPGS increases the number of MF

unimers compared to the MF micelles (Table 1), with an increase in the MF fraction (either in volume or mass) with the temperature, while the number of TPGS unimers in the micelles is reduced.

Table 3. Number of MF molecules (N_{MF}) and co-surfactant (TPGS or Tetronics, N_{CS}), volume and mass fraction of MF (ϕ_{MF} and w_{MF}) as deduced from SANS data analysis in the mixed systems (between parentheses, N_{agg} of the pure co-surfactant).

	$T / ^\circ C$	N_{CS}	N_{MF}	ϕ_{MF}	w_{MF}
1% TPGS + 0.2% MF	20	80 (118)	139	0.36	0.32
	37	69 (125)	161	0.43	0.39
	50	65 (125)	172	0.47	0.42
1% T904 + 0.2% MF	37	12 (24)	74	0.30	0.27
	50	20 (31)	77	0.21	0.19
1% T1107 + 0.2% MF	37	8 (11)	56	0.17	0.15
	50	14 (18)	78	0.15	0.13

3.2.2 Mixed Tetronic-MF micelles

As mentioned above, and in contrast to TPGS, Tetronic polymeric micelles are an interesting vehicle due to their capacity for pH-triggered delivery, conferred by the central diamine group. At moderately low concentrations, and above 35 °C, both T904 and T1107 form spherical micelles, with the core formed by the PPO blocks and the shell by the PEO blocks.^{28,30} Considering first the case of T904-MF mixed micelles, a distribution with hydrodynamic radius of 3.5 nm is observed at 20 °C (SI, Figure 5), similar to that of MF micelles ($R_h = 3.3$ nm, SI, Figure 1), while no presence of T904 unimers is detected. At 37 °C and 50 °C, micelles with a hydrodynamic radius of 5.2 nm are obtained (SI, Figure 5), slightly smaller than the T904 “pure” micelles under the same conditions ($R_h = 6$

nm).²⁸ When T1107 is combined with MF at 20 °C, larger sizes than those of T1107 unimers ($R_h = 3.3$ nm) and MF micelles are obtained, with 5.2 nm of radius (SI, Figure 6), indicating the incorporation of the T1107 unimers to the MF micelles. As the temperature increases, larger mixed micelles are obtained, with 7.0 nm hydrodynamic radius at 50 °C, yet smaller than “pure” T1107 micelles ($R_h = 8.0$ nm).³⁰ For both Tetronics (SI, Figures 5 and 6), a bimodal size distribution is obtained, with large and polydisperse aggregates with a hydrodynamic radius of ~ 100 nm, attributed to clusters of hydrophobic impurities of the poloxamines.^{39,40} Their mass fraction is negligible and, as the temperature increases, they dissolve in the mixed micelles.

When comparing the SANS patterns as a function of temperature in the absence or presence of MF, a similar trend to that of TPGS + MF can be observed, i.e. a slight reduction in the scattered intensity and a shift of the curves towards the high q regime (Figure 5). The structural parameters of the mixed micelles at 37 °C and 50 °C have been summarized in Table 4, corresponding to the fits to CSS-HS (Figure 5 and SI, Figure 7).

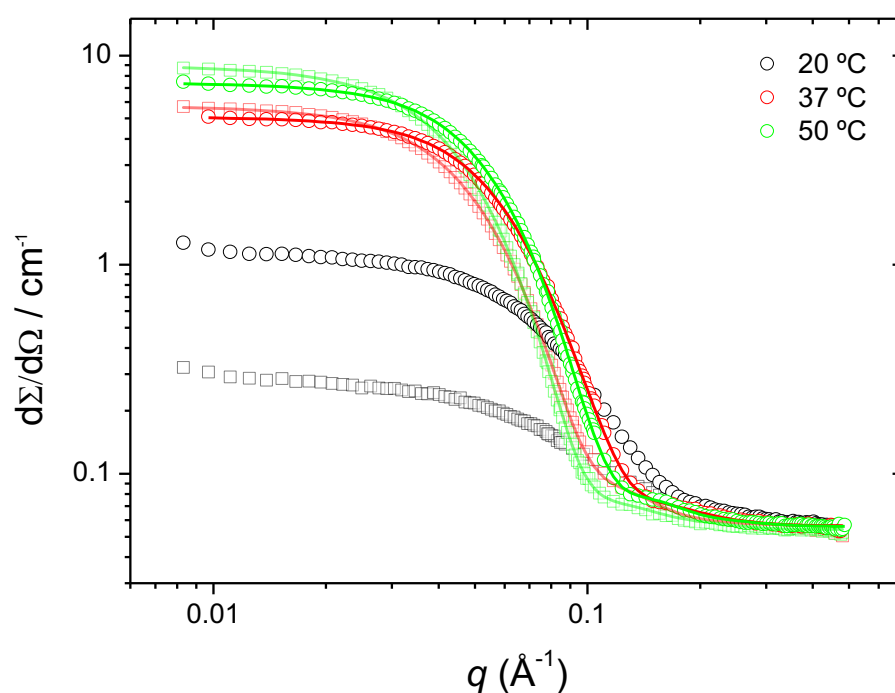


Figure 5. SANS curves of 1% T904 (□) and 1% T904 + 0.2% MF (○) in D₂O at 20, 37 and 50 °C. Solid lines correspond to the fits to CSS-HS model.

Table 4. Structural parameters of T904 and T1107 and MF in D₂O at deduced from SANS data analysis. R_c (core radius, Å), t (shell thickness, Å), ϕ (volume fraction), ρ_s (shell scattering length density $\times 10^6$ Å⁻²), ρ_c (core scattering length density $\times 10^6$ Å⁻²)

37 °C	R_c	t	ϕ	ρ_s	ρ_c
1% T904	39	26	0.020	6.34	0.344
1% T904 + MF 0.2%	30	24	0.032	6.04	-0.13
1% T1107	31	48	0.034	5.97	0.344
1% T1107 + MF 0.2%	28	46	0.049	6.03	-0.79

50 °C	R_c	t	ϕ	ρ_s	ρ_c
1% T904	39	25	0.021	5.79	0.344
1% T904 + MF 0.2%	34	22	0.030	5.91	0.02
1% T1107	37	46	0.031	5.80	0.344
1% T1107 + MF 0.2%	32	45	0.046	5.92	-0.41

The procedure used for the TPGS-MF system was also followed here. In this case, the sld_c of the Tetronic micelles alone was fixed to that of the pure PO ($\rho_{PO} = 3.44 \times 10^{-7}$ Å⁻²), in accordance with previous studies.^{28,30} The results for both Tetronics at 37 and 50 °C indicate a reduction in the size of the mixed micelles, in accordance with DLS data, as well as an increase in their volume fraction compared to the Tetronics alone. This evidence, and the lower or negative values of the sld_c obtained with the addition of MF, confirm the formation of the mixed micelles. No temperature effect (from 37 °C to 50 °C) is observed either in the size or the volume fraction of those mixed micelles (Table 4).

Once again, the interactions between the MF and the hydrophobic part of the co-surfactant that prove the formation of the mixed micelles are supported by NMR. The main changes in the proton spectra occur in the CH₃ signal of the hydrophobic tail of MF (1.07 ppm), which shifts to 1.11 ppm in the presence of the poloxamines, especially with T904 (SI, Figure 8), as well as the cross-peak in the 2D-NOESY spectrum between these protons and the CH₃ ones of the POs of the Tetronic (Figure 6). By contrast, methylene protons of the tail of MF (1.23 ppm) and the CH₃ of the hydrophilic head (3.44 ppm) of the MF shift in a lesser extent, while those of the EOs of the poloxamine do not shift at all (SI, Figure 8). This evidence and the absence of a clear cross-peak between the CH₃ protons of the MF polar head and those of the PPO block of the poloxamine in the 2D-NOESY, indicate that the MF zwitterion head must not be far from the micelle core, as it happens with TPGS.

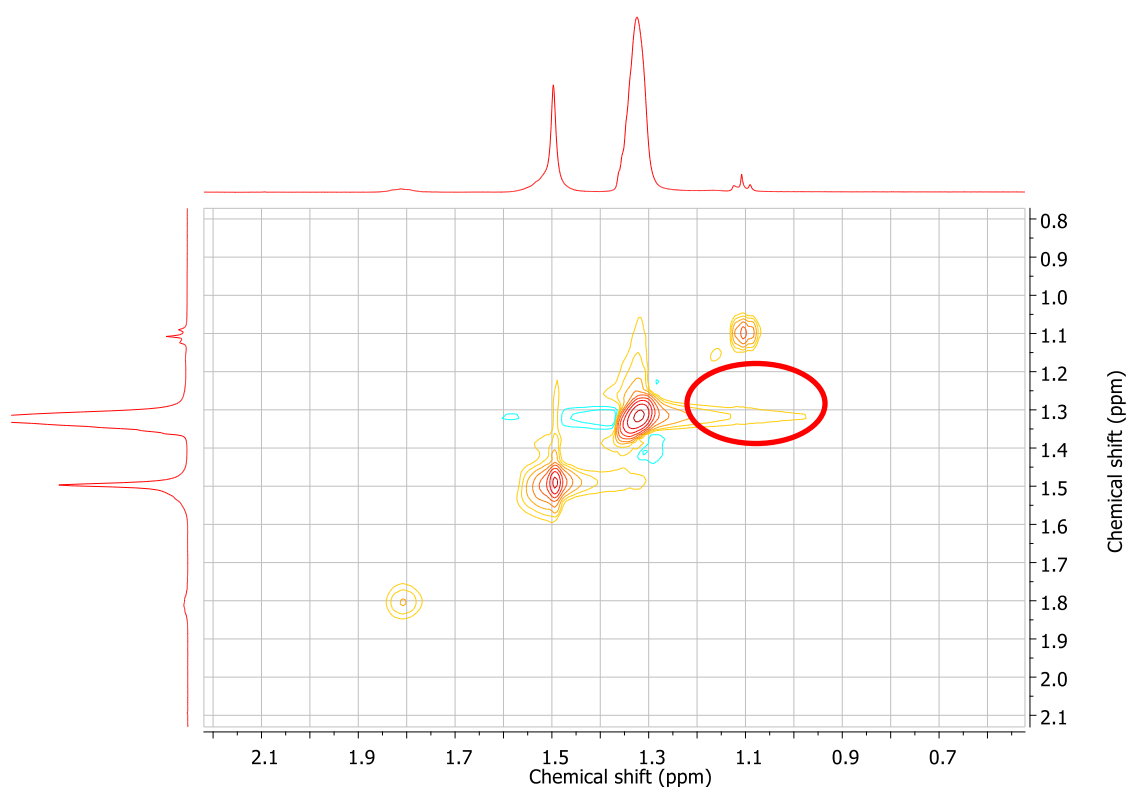


Figure 6. Magnification of the 2D-NOESY spectrum of 1% T904 + 0.2% MF at 50 °C.

The number of unimers of each surfactant in the mixed micelle can be calculated by solving the simultaneous equations (1) and (2), as it was done for TPGS+MF. The number water molecules per EO unit of the pure poloxamines at 37 °C are 21.7 and 23.9 for T904 (15 EO groups per arm) and T1107 (60 EO groups per arm), respectively. Values of 13.8 (T904) and 15.6 (T1107) are obtained at 50 °C from equation (3) and using the fitted values in Table 4. The results of these calculations (Table 3) show how the mixed micelles contain a relatively low proportion of MF (slightly less in the case of T1107) compared to TPGS. This is a direct consequence of the different structure and sizes of the hydrophobic moieties of TPGS (tocopherol) and the poloxamines (PPO blocks). While TPGS has a hydrophobic part similar to MF, in terms of mass and volume, Tetronic is larger and more flexible. Ideally, the more similar the hydrophobic moiety of the co-surfactants, the better compatibility and mixing.⁴¹ Regarding the temperature dependence, the number of Tetronic molecules in the mixed micelles increases for T904 and T1107 with the temperature, although a different MF composition is observed in each case. Thus, while in T904-MF micelles the number of MF unimers is virtually constant, T1107-MF micelles require higher temperatures to contain the same number of MF molecules (Table 3).

Poloxamine T1107 is larger and more hydrophilic than T904, with PEO blocks which are four times longer and PPO blocks which are almost the same length, and, thus, is capable of forming physical gels above 25% and 35 °C.³⁰ This opens the possibility of incorporating MF in the gels as a potential local way of delivery. Figure 7 shows the scattering patterns of 25% T1107 + 0.2% MF, with maxima at $q = 0.55, 0.77$ and 0.94 \AA^{-1} , which are typical of paracrystal structures formed by the packing of micelles. It can be seen how the curves of the mixed system practically match that of 25% T1107 in the absence of MF at any temperature (SI, Figure S9). Given the large difference in molar

volumes of both surfactants and considering that the molar ratio MF / T1107 is 0.29, a reduced number of MF molecules per micelle are expected in the dense packing of T1107 micelles, without significant changes in the gel structure. At 37 and 50 °C, conditions in which the poloxamine fully forms a gel (SI, Figure 9), the data analysis does not reveal any differences in the absence or presence of MF when fitting the SANS scattering pattern to a body-centred cubic paracrystalline (BCC) packing of spherical micelles, typical of these poloxamines.³⁰ The sphere radius is 34 Å, practically matching the core of the T1107 micelles, and the cell parameter, a , of the paracrystal is 161 Å. Therefore, the packing appears to consist of a BCC network of polydisperse spheres containing mainly PPO. The PEO shells expand up to a total micelle radius of 70 Å, according to the calculated dimensions of the paracrystal cell ($R_{mic}=\sqrt{3}/4a$), which is slightly lower than the size of the micelles at low concentration (Table 4). This would imply a certain extent of overlapping of the coronas of adjacent micelles, which has also been observed in the larger Tetronic 908 (114 EOs and 21 POs per arm.³¹)

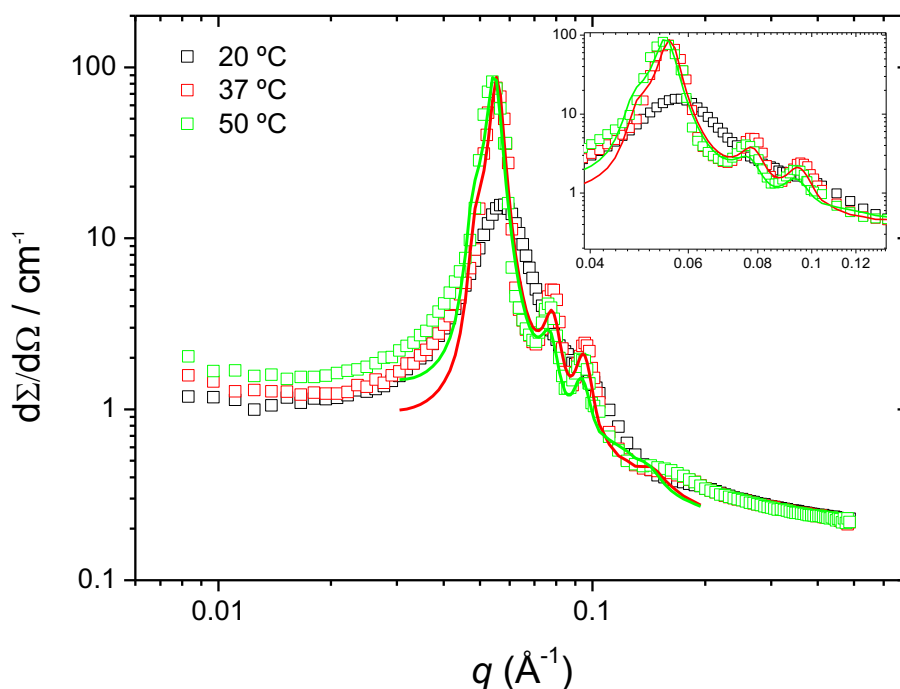


Figure 7. SANS curves of 25% T1107 + 0.2% MF in D₂O at 20, 37 and 50 °C. Solid lines correspond to the fits to a BCC paracrystal.

3.3 Biological evaluation of MF-loaded polymeric micelles

After characterizing the structural features of the different MF-cosurfactant systems, we have tested their activity against *L. major* promastigotes. The MTT test, a colorimetric assay for assessing cell metabolic activity, was performed to determine the cytotoxicity of the selected formulations (Table 5). It can be seen how the EC₅₀ of MF alone is 10.63 ± 3.65 µM, while TPGS, T904 and T1107 are not active against *L. major* promastigotes, with EC₅₀ values higher than 50 µM. Most interestingly, the combination of the three surfactants with MF makes the drug more active than MF alone. In fact, the EC₅₀ of the formulation T904-MF is significantly lower (*p<0.05) than that of MF alone, proving to be the most active system in the extracellular form of parasites.

Table 5. EC₅₀ values of studied MF micelles on *L. major* promastigotes 72 hours post-treatment.

Effect against <i>Leishmania major</i> promastigotes viability	
Formulations	EC ₅₀ (mean ± SD)
MF	10.63 ± 3.65 µM
TPGS	>100 µM
TPGS-MF	6.82 ± 0.75 µM
T904	>50 µM
T904-MF	6.13 ± 1.12 µM (*)
T1107	>50 µM
T1107-MF	7.01 ± 0.47 µM

With these results and considering that T904-MF, T1107-MF and TPGS-MF systems do not exhibit toxicity against murine macrophages (data not shown), we were prompted to assess their activity against *L. major* intracellular amastigotes. *L. major*-infected

macrophages were then exposed to different formulations. For each copolymer, surfactant, surfactant-MF (5 μ M) and surfactant-MF (10 μ M), as well as MF alone (5 μ M and 10 μ M) samples were studied, where the concentrations 5 and 10 μ M correspond to a 1000 and 500 dilution of the stock solution (1% surfactant + 0.2% MF), respectively. The results obtained for T904 and T1107 are compared in Figure 8. Very interestingly, the activity of T904-MF results considerably higher than that of MF alone, especially at low concentrations of the drug. However, no significant difference is observed in the presence or absence of T1107. A possible explanation could be related to the actual concentration of the surfactants in the bioassays and the dilution effect. While T904-MF mixed micelles are completely formed at 37 °C at 1% T904 + 0.2% MF (Table 3), under the biological studies conditions, T904-MF mixed micelles can be formed even at the lower concentration used (MF 5 μ M), favoring the entrance of MF in infected macrophages. Instead, the larger T1107 requires higher temperatures than 37 °C to fully form micelles and their composition varies from 37 °C to 50 °C,^{28,30} as observed in Table 3. T1107 is then less prone to self-aggregate at 37 °C and, at the concentrations used for biological studies, the formation of mixed T1107-MF micelles may not occur, or it is scarce. MF micelles may coexist with T1107 unimers, producing nearly the same activity as observed for MF micelles (Figure 8). However, while this temperature effect may explain the biological results for the Tetronic-MF systems, it would not justify the lack of response of the TPGS-MF one, as shown in SI, Figure 10. Mechanisms other than the mentioned dilution effect or micelle structure-MF load must be involved.

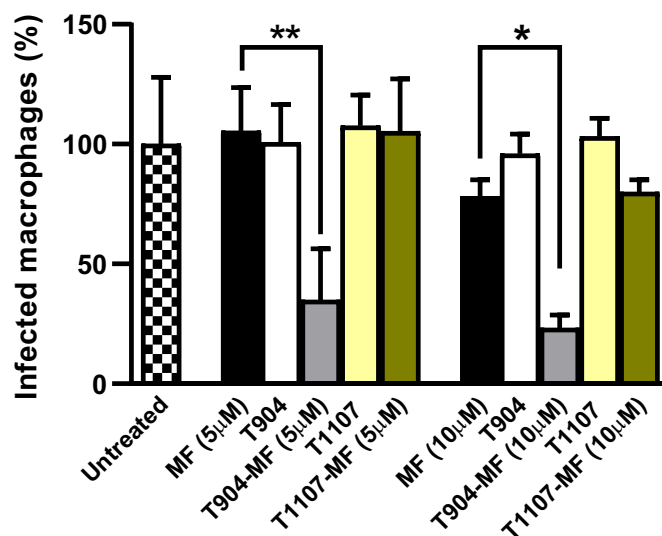


Figure 8: Effect of MF, T904, T1107, T904-MF and T1107-MF on *L. major*- infected peritoneal macrophages. Treatments were performed at 5 and 10 µM of MF. Bars represent the percentage of infected macrophages with *L. major* after 72 h of treatment.

4. Conclusions

The combination of MF, a zwitterionic amphiphile used as anti-leishmanial drug, with three polymeric non-ionic surfactants (TPGS, T904 and T1107) to form mixed micelles and gels has been investigated. SANS and DLS studies on MF micelles reveal that the drug self-aggregates into core-shell spheres. The micelles are thermally stable, with a slight decrease in aggregation number as temperature increases and no concentration effects on the structure from 0.2% to 1% of the drug.

Combined SANS and NMR experiments show that spherical core-shell mixed micelles form when combining MF and the three polymeric co-surfactants over a wide range of temperatures. For all the surfactants studied, mixed micelles are formed where the hydrophobic parts (PPO blocks for Tetronics and tocopherol moiety for TPGS) are in close contact with the hydrophobic tail of MF, and micelles contain a highly hydrated hydrophilic shell mainly formed by the PEOs. With the Tetronic copolymer, certain

differences with implications in the biological activity are observed depending on the block length of the Tetronics. In T904-MF, the number of MF molecules per mixed micelle is independent of temperature and micelles are fully formed at 37 °C, while T1107-MF requires higher temperatures (50 °C) to reach the same number of MF molecules. In both cases, lower aggregation numbers are obtained compared to MF micelles. At high concentrations of T1107 (> 20%), the gelation of the system occurs, revealing a BCC internal structure of the gel, without significant influences on the structure at 0.2% of the drug. By contrast, the number of MF molecules increases in TPGS-MF mixed micelles compared to MF micelles, observing an enhancement in the MF weight fraction with the temperature.

Biological studies with extracellular promastigotes have been performed, observing a reduction of the EC₅₀ of the MF for all the formulations compared to MF alone, more noticeable in the T904-MF system. Effectiveness of T904-MF composition is also observed in intracellular amastigotes, allowing a significant higher activity of the MF, especially at low concentrations of the drug (5 µM), while no effect of the surfactant is observed when using T1107 and TPGS. This is ascribed to the full formation of mixed micelles under biological conditions which is attained with T904-MF system. Hence, the combination of MF with poloxamines as co-surfactants to form mixed polymeric micelles seems a promising formulation for leishmaniasis treatment, in particular when more hydrophobic Tetronics, like T904, are used,.

Conflict of interests

The authors declare that they have no competing interests.

Acknowledgements

The authors gratefully acknowledge the financial support provided by MINECO (Project MAT2014-59116-C2-2-R), Obra Social La Caixa (LCF/PR/PR13/11080005) and Fundación Caja Navarra, Gobierno Navarra Salud (12/2017), Fundación Roviralta, Ubesol, Government of Navarre, Laser Ebro, and Fundación Garcilaso de la Vega. JCNS is acknowledged for the access to the KWS-2 diffractometer at the Heinz Maier-Leibnitz Zentrum (MLZ), Garching, Germany. J.P-R. also acknowledges the Asociación de Amigos de la Universidad de Navarra for his doctoral grant. This work benefited from the use of the SasView application, originally developed under NSF award DMR-0520547. SasView contains code developed with funding from the European Union's Horizon 2020 research and innovation program under the SINE2020 project, grant agreement No 654000.

References

- (1) Fernández-Rubio, C.; Larrea, E.; Peña-Guerrero, J.; Sesma-Herrero, E.; Gamboa, I.; Berrio, C.; Plano, D.; Amin, S.; Sharma, A. K.; Nguewa, P. A. Leishmanicidal Activity of Isoselenocyanate Derivatives. *Antimicrob. Agents Chemother.* **2019**, 63 (2), 1–12.
- (2) David, C. V.; Craft, N. Cutaneous and Mucocutaneous Leishmaniasis. *Dermatol. Ther.* **2009**, 22 (6), 491–502.
- (3) Fuertes, M. A.; Nguewa, P. A.; Castilla, J.; Alonso, C.; Perez, J. M. Anticancer Compounds as Leishmanicidal Drugs: Challenges in Chemotherapy and Future Perspectives. *Curr. Med. Chem.* **2008**, 15 (5), 433–439.
- (4) Shukla, A. K.; Patra, S.; Dubey, V. K. Evaluation of Selected Antitumor Agents as Subversive Substrate and Potential Inhibitor of Trypanothione Reductase: An Alternative Approach for Chemotherapy of Leishmaniasis. *Mol. Cell. Biochem.* **2011**, 352 (1–2), 261–270.
- (5) Vinson, R. Application for Inclusion of Miltefosine on WHO Model List of Essential Medicines. *Paladin Labs.* **2010**, 21.
- (6) Kapil, S.; Singh, P. K.; Silakari, O. An Update on Small Molecule Strategies

- Targeting Leishmaniasis. *European Journal of Medicinal Chemistry*. Elsevier Masson SAS September 5, 2018, pp 339–367.
- (7) Nazari-Vanani, R.; Dehdari-Vais, R.; Sharifi, F.; Sattarahmady, N.; Karimian, K.; Motazedian, M. H.; Heli, H. Investigation of Anti-Leishmanial Efficacy of Miltefosine and Ketoconazole Loaded on Nanoniosomes. *Acta Trop.* **2018**, *185*, 69–76.
 - (8) Van Bocxlaer, K.; Yardley, V.; Murdan, S.; Croft, S. L. Topical Formulations of Miltefosine for Cutaneous Leishmaniasis in a BALB/c Mouse Model. *J. Pharm. Pharmacol.* **2016**, *68* (7), 862–872.
 - (9) Gontijo-Aguiar, M.; Machado-Pereira, A. M.; Fernandes, A. P.; Miranda-Ferreira, L. A. Reductions in Skin and Systemic Parasite Burdens as a Combined Effect of Topical Paromomycin and Oral Miltefosine Treatment of Mice Experimentally Infected with Leishmania (Leishmania) Amazonensis. *Antimicrob. Agents Chemother.* **2010**, *54* (11), 4699–4704.
 - (10) Soto, J.; Rea, J.; Balderrama, M.; Toledo, J.; Soto, P.; Valda, L.; Berman, J. D. Short Report: Efficacy of Miltefosine for Bolivian Cutaneous Leishmaniasis. *Am. J. Trop. Med. Hyg.* **2008**, *78* (2), 210–211.
 - (11) Soto, J.; Arana, B. A.; Toledo, J.; Rizzo, N.; Vega, J. C.; Diaz, A.; Luz, M.; Gutierrez, P.; Arboleda, M.; Berman, J. D.; et al. Miltefosine for New World Cutaneous Leishmaniasis. *Clin. Infect. Dis.* **2004**, *38* (9), 1266–1272.
 - (12) Sundar, S.; Jha, T. K.; Thakur, C. P.; Bhattacharya, S. K.; Rai, M. Oral Miltefosine for the Treatment of Indian Visceral Leishmaniasis. *Trans. R. Soc. Trop. Med. Hyg.* **2006**, *100*, 26–33.
 - (13) Sundar, S.; Makharia, A.; More, D. K.; Agrawal, G.; Voss, A.; Fischer, C.; Bachmann, P.; Murray, H. W. Short-Course of Oral Miltefosine for Treatment of Visceral Leishmaniasis. *Clin. Infect. Dis.* **2000**, *31* (4), 1110–1113.
 - (14) Verma, N. K.; Dey, C. S. Possible Mechanism of Miltefosine-Mediated Death of Leishmania Donovanii. *Antimicrob. Agents Chemother.* **2004**, *48* (8), 3010–3015.
 - (15) Wasunna, M.; Njenga, S.; Balasegaram, M.; Alexander, N.; Omollo, R.; Edwards, T.; Dorlo, T. P. C.; Musa, B.; Ali, M. H. S.; Elamin, M. y.; et al. Efficacy and Safety of AmBisome in Combination with Sodium Stibogluconate or Miltefosine and Miltefosine Monotherapy for African Visceral Leishmaniasis: Phase II Randomized Trial. *PLoS Negl. Trop. Dis.* **2016**, *10* (9), 1–18.
 - (16) Sindermann, H.; Engel, J. Development of Miltefosine as an Oral Treatment for

- Leishmaniasis. *Trans. R. Soc. Trop. Med. Hyg.* **2006**, *100*, 17–20.
- (17) Calogeropoulou, T.; Angelou, P.; Detsi, A.; Fragiadaki, I.; Scoulica, E. Design and Synthesis of Potent Antileishmanial Cycloalkylidene-Substituted Ether Phospholipid Derivatives. *J. Med. Chem.* **2008**, *51* (4), 897–908.
 - (18) Pachioni-Vasconcelos, J. D. A.; Lopes, A. M.; Apolinário, A. C.; Valenzuela-Oses, J. K.; Costa, J. S. R.; Nascimento, L. D. O.; Pessoa, A.; Barbosa, L. R. S.; Rangel-Yagui, C. D. O. Nanostructures for Protein Drug Delivery. *Biomaterials Science*. Royal Society of Chemistry February 1, 2016, pp 205–218.
 - (19) Valenzuela-Oses, J. K.; García, M. C.; Feitosa, V. A.; Pachioni-Vasconcelos, J. A.; Gomes-Filho, S. M.; Lourenço, F. R.; Cerize, N. N. P.; Bassères, D. S.; Rangel-Yagui, C. O. Development and Characterization of Miltefosine-Loaded Polymeric Micelles for Cancer Treatment. *Mater. Sci. Eng. C* **2017**, *81* (July), 327–333.
 - (20) Feitosa, V. A.; de Almeida, V. C.; Malheiros, B.; de Castro, R. D.; Barbosa, L. R. S.; Cerize, N. N. P.; Rangel-Yagui, C. D. O. Polymeric Micelles of Pluronic F127 Reduce Hemolytic Potential of Amphiphilic Drugs. *Colloids Surfaces B Biointerfaces* **2019**, *180*, 177–185.
 - (21) Alexandridis, P.; Hatton, T. A. Poly(ethylene Oxide)-Poly(propylene Oxide)-Poly(ethylene Oxide) Block Copolymer Surfactants in Aqueous Solutions and at Interfaces: Thermodynamics, Structure, Dynamics, and Modeling. *Colloids and Surfaces A: Physicochemical and Engineering Aspects*. March 10, 1995, pp 1–46.
 - (22) Su, Y. L.; Wang, J.; Liu, H. Z. FTIR Spectroscopic Investigation of Effects of Temperature and Concentration on PEO-PPO-PEO Block Copolymer Properties in Aqueous Solutions. *Macromolecules* **2002**, *35* (16), 6426–6431.
 - (23) Nagarajan, R. Solubilization of Hydrocarbons and Resulting Aggregate Shape Transitions in Aqueous Solutions of Pluronic® (PEO-PPO-PEO) Block Copolymers. *Colloids Surfaces B Biointerfaces* **1999**, *16* (1–4), 55–72.
 - (24) Sadoqi, M.; Lau-Cam, C. A.; Wu, S. H. Investigation of the Micellar Properties of the Tocopheryl Polyethylene Glycol Succinate Surfactants TPGS 400 and TPGS 1000 by Steady State Fluorometry. *J. Colloid Interface Sci.* **2009**, *333* (2), 585–589.
 - (25) Zhang, Z.; Tan, S.; Feng, S.-S. Vitamin E TPGS as a Molecular Biomaterial for Drug Delivery. *Biomaterials* **2012**, *33* (19), 4889–4906.

- (26) Guo, Y.; Luo, J.; Tan, S.; Oketch, B.; Zhang, Z. The Applications of Vitamin E TPGS in Drug Delivery. *Eur. J. Pharm. Sci.* **2013**, *49* (2), 175–186.
- (27) Puig-Rigall, J.; Grillo, I.; Dreiss, C. A.; González-Gaitano, G. Structural and Spectroscopic Characterization of TPGS Micelles: Disruptive Role of Cyclodextrins and Kinetic Pathways. *Langmuir* **2017**, *33* (19), 4737–4747.
- (28) González-Gaitano, G.; Müller, C.; Radulescu, A.; Dreiss, C. A. Modulating the Self-Assembly of Amphiphilic X-Shaped Block Copolymers with Cyclodextrins: Structure and Mechanisms. *Langmuir* **2015**, *31* (14), 4096–4105.
- (29) González-Gaitano, G.; da Silva, M. A.; Radulescu, A.; Dreiss, C. A. Selective Tuning of the Self-Assembly and Gelation of a Hydrophilic Poloxamine by Cyclodextrins. *Langmuir* **2015**, *31* (20), 5645–5655.
- (30) Serra-Gómez, R.; Dreiss, C. A.; González-Benito, J.; González-Gaitano, G. Structure and Rheology of Poloxamine T1107 and Its Nanocomposite Hydrogels with Cyclodextrin-Modified Barium Titanate Nanoparticles. *Langmuir* **2016**, *32* (25), 6398–6408.
- (31) Puig-Rigall, J.; Obregon-Gomez, I.; Monreal-Pérez, P.; Radulescu, A.; Blanco-Prieto, M. J.; Dreiss, C. A.; González-Gaitano, G. Phase Behaviour, Micellar Structure and Linear Rheology of Tetra-block Copolymer Tetronic 908. *J. Colloid Interface Sci.* **2018**, *524*, 42–51.
- (32) Radulescu, A.; Szekely, N. K.; Appavou, M. S.; Pipich, V.; Kohnke, T.; Ossovyi, V.; Staringer, S.; Schneider, G. J.; Amann, M.; Zhang-Haagen, B.; et al. Studying Soft-Matter and Biological Systems over a Wide Length-Scale from Nanometer and Micrometer Sizes at the Small-Angle Neutron Diffractometer KWS-2. *J. Vis. Exp.* **2016**, No. 118, e54639.
- (33) Macdonald, P. M.; Rydall, J. R.; Kuebler, S. C.; Winnik, F. M. Synthesis and Characterization of a Homologous Series of Zwitterionic Surfactants Based on Phosphocholine. *Langmuir* **1991**, *7* (11), 2602–2606.
- (34) Yaseen, M.; Lu, J. R.; Webster, J. R. P.; Penfold, J. The Structure of Zwitterionic Phosphocholine Surfactant Monolayers. *Langmuir* **2006**, *22* (13), 5825–5832.
- (35) Rakotomanga, M.; Loiseau, P. M.; Saint-Pierre-Chazalet, M. Hexadecylphosphocholine Interaction with Lipid Monolayers. *Biochim. Biophys. Acta - Biomembr.* **2004**, *1661* (2), 212–218.
- (36) Lukac, M.; Mrva, M.; Garajova, M.; Mojziso, G.; Varinska, L.; Mojzis, J.; Sabol, M.; Kubincova, J.; Haragova, H.; Ondriska, F.; et al. Synthesis, Self-

- Aggregation and Biological Properties of Alkylphosphocholine and Alkylphosphohomocholine Derivatives of Cetyltrimethylammonium Bromide, Cetylpyridinium Bromide, Benzalkonium Bromide (C16) and Benzethonium Chloride. *Eur. J. Med. Chem.* **2013**, *66*, 46–55.
- (37) Sanchez-Fernandez, A.; Moody, G. L.; Murfin, L. C.; Arnold, T.; Jackson, A. J.; King, S. M.; Lewis, S. E.; Edler, K. J. Self-Assembly and Surface Behaviour of Pure and Mixed Zwitterionic Amphiphiles in a Deep Eutectic Solvent. *Soft Matter* **2018**, *14* (26), 5525–5536.
- (38) Valero, M.; Castiglione, F.; Mele, A.; da Silva, M. A.; Grillo, I.; González-Gaitano, G.; Dreiss, C. A. Competitive and Synergistic Interactions between Polymer Micelles, Drugs, and Cyclodextrins: The Importance of Drug Solubilization Locus. *Langmuir* **2016**, *32* (49), 13174–13186.
- (39) Polik, W. F.; Burchard, W. Static Light Scattering from Aqueous Poly(ethylene Oxide) Solutions in the Temperature Range 20–90 °C. *Macromolecules* **1983**, *16* (6), 978–982.
- (40) Brown, W. Diffusion of Poly(ethylene Oxide) in Semidilute Aqueous Solution: Dynamic Light Scattering and Gradient Diffusion. *Polymer (Guildf)*. **1985**, *26* (11), 1647–1650.
- (41) Moroi, Y. Mixed Micelle Formation. In *Micelles*; Springer US: Boston, MA, 1992; pp 183–194.